GEOSCIENCE FRONTIERS 3(5) (2012) 707–715

available at www.sciencedirect.com

China University of Geosciences (Beijing)

GEOSCIENCE FRONTIERS

journal homepage: www.elsevier.com/locate/gsf

RESEARCH PAPER

End Late Paleozoic tectonic stress field in the southern edge of Junggar Basin

Wei Ju [a,b], Guiting Hou [a,b,*], Le Li [a], Fangfeng Xiao [a]

[a] *The Key Laboratory of Orogenic Belts and Crustal Evolution, Ministry of Education, School of Earth and Space Science, Peking University, Beijing 100871, China*

[b] *Institute of Oil and Gas Research, Peking University, Beijing 100871, China*

Received 19 September 2011; accepted 8 December 2011
Available online 30 December 2011

KEYWORDS
Tectonic stress field;
Junggar Basin;
End Late Paleozoic;
Stress-response structures;
Stress regime

Abstract This paper presents the end Late Paleozoic tectonic stress field in the southern edge of Junggar Basin by interpreting stress-response structures (dykes, folds, faults with slickenside and conjugate joints). The direction of the maximum principal stress axes is interpreted to be NW–SE (about 325°), and the accommodated motion among plates is assigned as the driving force of this tectonic stress field. The average value of the stress index R' is about 2.09, which indicates a variation from strike-slip to compressive tectonic stress regime in the study area during the end Late Paleozoic period. The reconstruction of the tectonic field in the southern edge of Junggar Basin provides insights into the tectonic deformation processes around the southern Junggar Basin and contributes to the further understanding of basin evolution and tectonic settings during the culmination of the Paleozoic.

© 2011, China University of Geosciences (Beijing) and Peking University. Production and hosting by Elsevier B.V. All rights reserved.

* Corresponding author. The Key Laboratory of Orogenic Belts and Crustal Evolution, Ministry of Education, School of Earth and Space Science, Peking University, Beijing 100871, China. Tel.: +86 13521511918.

E-mail address: gthou@pku.edu.cn (G. Hou).

1674-9871 © 2011, China University of Geosciences (Beijing) and Peking University. Production and hosting by Elsevier B.V. All rights reserved.

Peer-review under responsibility of China University of Geosciences (Beijing).
doi:10.1016/j.gsf.2011.12.007

1. Introduction

Models on tectonic deformation processes require an understanding of the tectonic stress state (Wan, 1988; Hou et al., 2010a,b). Besides, analysis of tectonic stress field has various applications including the migration and accumulation of hydrocarbon deposits (Cao, 2005; Zhang et al., 2007).

Junggar is a triangular-shaped area bordered by the Tianshan range in the south, the Altai in the northeast and the west Junggar mountains in the northwest, with different orientations of verging and accretionary events (Charvet et al., 2007; Xiao et al., 2008; Choulet et al., in press; Pirajno et al., 2011; Xiao et al., 2011; Zhang et al., 2011). The reconstruction of the tectonic stress field during the end Late Paleozoic in the southern edge of Junggar Basin is of importance for the

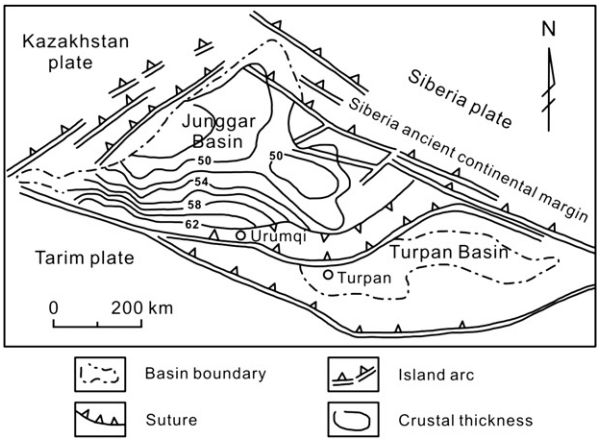

Figure 1 Sketch map of the tectonic framework of the Junggar Basin (after Chen and Wang, 2004).

analysis of tectonic deformation processes around the southern Junggar Basin during that period.

2. Geological setting

The Junggar Basin, with an area of about 130,000 km^2, is located in the northern part of Xinjiang, at the convergence area among the Kazakhstan plate, Siberia plate and Tarim plate. The region forms a triangle-shaped sedimentary basin surrounded by Paleozoic orogenic belts (Xiao, 1992; Han et al., 1999; Chen and Wang, 2004; Chen et al., 2005; Fig. 1).

The Hercynian movement in the Carboniferous caused the seas surrounding the Junggar to close by plate convergence. The earlier sedimentary and volcanic rocks were folded and constituted the basement of the Junggar Basin (Wang and Chen, 2004). Previous studies have shown that the Junggar Basin was under the collision to basin formation stage during Carboniferous to the end of Permian period (Chen et al., 2002; Wu et al., 2005; Yang et al., in press). During the Early–Middle Carboniferous, the Siberian plate collided with the Junggar, which started the development stage of foreland basin systems in the eastern Junggar. To the northwest of Junggar Basin was a passive continental margin during the Devonian to Early Carboniferous, which witnessed the collision of the Junggar and Kazakhstan plates in the Middle or even Late Carboniferous. Finally, the Junggar collided with the Tarim plate in the Late Carboniferous to Early Permian, which started the evolution of thrusts in the North Tianshan Mountains and the southern foreland basin system (Zhang, 1995; Chen and Wang, 2004; Wang and Chen, 2004; Chen et al., 2005; Wu et al., 2005; Geng et al., 2009; Zhang et al., 2011). Thus, before the end of Permian, the Junggar terrain was bonded together with Kazakhstan plate, Siberia plate and Tarim plate (Xiao, 1992; Han et al., 1999; Chen et al., 2005); and the basic tectonic styles can be summarized as arc-arc collision, oroclinal bending and large-scale rotation, and multiple subductions with a complicated archipelago paleogeography (Xiao et al., 2010).

The present study area is around Urumqi city (Fig. 2) with two transects along the Fukang–Tianchi route and the Urumqi–Tuoli route (Fig. 2).

3. Structural analysis and palaeostress reconstruction

3.1. Dykes

The palaeostress field is not very easy to reconstruct because few palaeostress indicators remain (Hou et al., 2010a). Mafic dyke

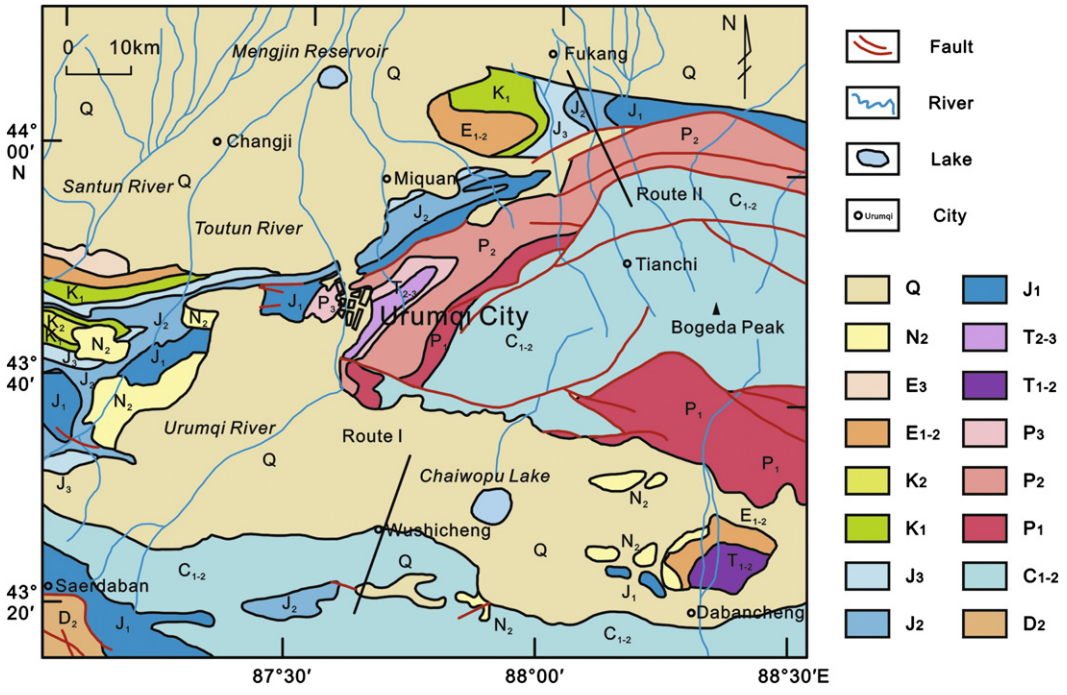

Figure 2 Geological map of the Urumqi area, Xinjiang Uygur Autonomous Region.

Figure 3 Stress-response structures in the study area. a: conjugate joints in the Urumqi–Tuoli route; b: fault plane with slickenside (the pen indicates the movement direction of the opposite wall); c: dykes in Tuoli County, the strike is NW–SE direction.

swarms represent conspicuous extensional structures and are of great current international interest, because they are excellent time makers and palaeostress indicators, and can be used to reconstruct the palaeostress field (Ernst et al., 1995, 2001; Hou et al., 2006; Hou, in press). In general, the maximum (σ_1) and intermediate (σ_2) principal compressive stress directions lie normal to one another within the plane of the dyke, whereas the minimum principal compressive stress (σ_3) is perpendicular to the plane of the dyke (Hoek and Seitz, 1995; Gudmundsson, 1995; Ray et al., 2007; Hou et al., 2010a,b).

The dykes represent small extensional fractures or weak planes that were formed under tectonic stress. Subsequently, these small extensional fractures or weakness planes extended successively, and finally they were intruded by mafic magma leading to the formation of the dykes. The undeformed and unmetamorphosed mafic dykes are usually vertical, with stable strike and are of great importance in geological comparison (Hou et al., 2005; Xiao et al., 2009).

A series of mafic dyke swarms, generally parallel, are well developed in the North Tianshan area. The dykes are typical dolerites and algovites, and most of the dykes are subvertical without deformation and metamorphism. K-Ar dating shows that they were formed in the Late Permian (National Geoscience Database, www.geoscience.cn). The Tuoli dyke swarm (Fig. 3c), 60–80 km south of Urumqi city, is vertical or slightly east dipping (Figs. 3 and 4). From the rose diagram of these dykes, the average strike is estimated as 326 degrees (Fig. 4), which indicates the maximum principal compressive stress direction is NW–SE (about 326 degrees, Xiao et al., 2009).

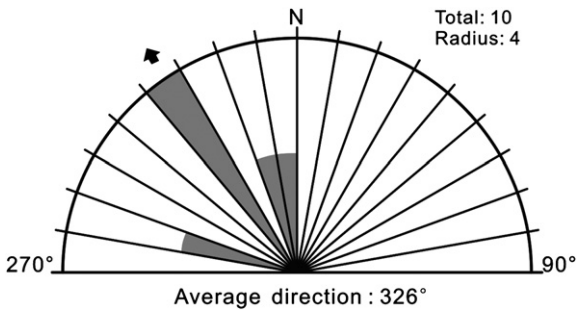

Figure 4 Rose diagram of the strike of dyke swarms in Tuoli County.

3.2. Folds

β analysis of the fold limbs provides an average estimate of the trends of the axial plane and limbs, which further indicates the direction of the maximum principal stress axes. In general, the occurrence of axial plane is perpendicular to the maximum principal compressive stress direction when the folds are simple and the axial planes are almost vertical (Ramsay and Huber, 1987; Wan, 1988; Xiao et al., 2009). In a subduction to collision setting, as in the Junggar Basin, folds may initially develop due to buckling (strictly pure shear type), but non-coaxial deformation may lead to reorientation of folds.

Table 1 Palaeostress tensors from stress-response structures data in Fukang–Tianchi route.

Site	Location		Data type	Stratigraphic position	Principal stress axes	Dip direction (°)	Dip angle (°)	*n*	*R*	Graphical solution
	Longitude (E)	Latitude (N)								
FT01	88°07′30″	43°54′18″	1	C–P	σ_1	328	17	18	0.52	Fig. 5a
					σ_2	066	23			
					σ_3	204	60			
FT02	88°07′51″	43°54′00″	1	C–P	σ_1	319	15	13	0.49	Fig. 5b
					σ_2	056	27			
					σ_3	203	58			
FT03	88°04′48″	43°57′36″	2	C–P	σ_1	333	06	10	0.56	Fig. 5c
					σ_2	176	82			
					σ_3	063	02			
FT04	88°04′57″	43°57′36″	3	J						Fig. 5d
FT05	88°04′50″	43°57′40″		J	σ_1	352.6	15.2	40		
FT06	88°04′32″	43°57′47″		J	σ_2					
FT07	88°04′44″	43°57′42″		J	σ_3					
FT08	88°03′40″	44°00′12″		J						
FT09	88°03′40″	44°00′24″	3	J	σ_1	163.3	13.4	35		Fig. 5e
FT10	88°04′04″	44°01′10″		J	σ_2					
FT11	88°04′12″	43°01′50″		J	σ_3					

σ_1: maximum principal compressive stress; σ_2: intermediate principal compressive stress; σ_3: minimum principal compressive stress. Date type: 1 – fault plane with slickenside; 2 – conjugate joints; 3 – folds; R – the ratio of principal stress differences; $R = (\sigma_2 - \sigma_3)/(\sigma_1 - \sigma_3)$; C–P for Carboniferous–Permian and J for Jurassic.

In the field, we measured and obtained data from 75 folds and divided them into two groups based on their locations. The average angle of axial planes is about 75 degrees, from which we could estimate the maximum principal compressive stress direction (Table 1).

3.3. Faults and conjugate joints

Filed investigation on the kinematics was conducted in the study area and the palaeostress tensors were obtained by the application of a stress inversion technique (described in Delvaux and Sperner, 2003) on fault measurements and conjugate joints (Fig. 3a and b).

The inversion method is based on the assumption that (a) the stress field is uniform and invariant in space and time, and (b) slip on a plane occurs in the direction of the maximum resolved shear stress (Bott, 1959; Etchecopar et al., 1981; Delvaux and Barth, 2010). Striae on a fault plane, such as slickenside lineations (Fig. 3b), may be used to infer the sense of relative movement between the footwall block and the hanging wall block of a fault (Doblas, 1998). Slickensides thus provide the essential tool for stress tensor calculations based on the assumption mentioned above and parameters computed of the reduced stress tensor, as defined by Angelier (1989): the principal stress axes σ_1 (maximum compression), σ_2 (intermediate compression) and σ_3 (minimum compression), and the ratio of principal stress differences $R = (\sigma_2 - \sigma_3)/(\sigma_1 - \sigma_3)$ (Angelier, 1979; Delvaux et al., 1995; Manby and Lyberis, 1996). The four parameters are determined using successively improved version of the Right Dihedron method and a rotational optimization method (Delvaux and Sperner, 2003). These two methods have been successfully applied in many regions (Delvaux, 1993; Delvaux et al., 1995; Zaineldeen et al., 2002; Foeken et al., 2006; Ferroni et al., 2008).

The method also allows the use of compressional and tensional joints for estimating the four parameters of the stress tensor. However, as to conjugate joints, if the strata are horizontal, we can calculate them directly. If not, the strata leveling must be done before analysis (Rawnsley et al., 1998; Arlegui and Simon, 2001; Eyal et al., 2001). The data in this paper have been adjusted by using the StereoNet program (Version 3.06).

In the field, we measured and obtained 41 faults with slickensides data, divided them into three groups, calculated them with the method described in Delvaux and Sperner (2003) (Fig. 5), and the palaeostress tensors were obtained (Table 1).

3.4. Palaeostress reconstruction

The palaeostress reconstruction in the study area is conducted along the Fukang–Tianchi route and Urumqi–Tuoli route with the rotational optimization method (described in Delvaux and Sperner, 2003; Table 1; Figs. 5 and 6).

The fault and slickensides are well developed in the Carboniferous–Permian strata in the North Bogeda Mountain and South Tuoli County, which are not seen in the Triassic–Quaternary strata. Furthermore, the Mesozoic and Cenozoic tectonic stress fields were established in this area, with the maximum principal stress (compression) direction as near N–S and NE–NNE (Tao, 1992; Wu et al., 2000; Xiao et al., 2009). Therefore the end Late Paleozoic tectonic stress field could be confirmed and reconstructed (NW–SE direction; Table 1 and Fig. 5).

The conjugate joints developed in the Carboniferous–Permian strata also record this stress field (Table 1; Figs. 5 and 6). The age of the dyke swarm in this area also define an end Late Paleozoic stress field (Fig. 4). However, the folds occur in the Jurassic strata, and therefore they represent tectonic deformation which is broadly contemporaneous with or younger than Jurassic. These folds

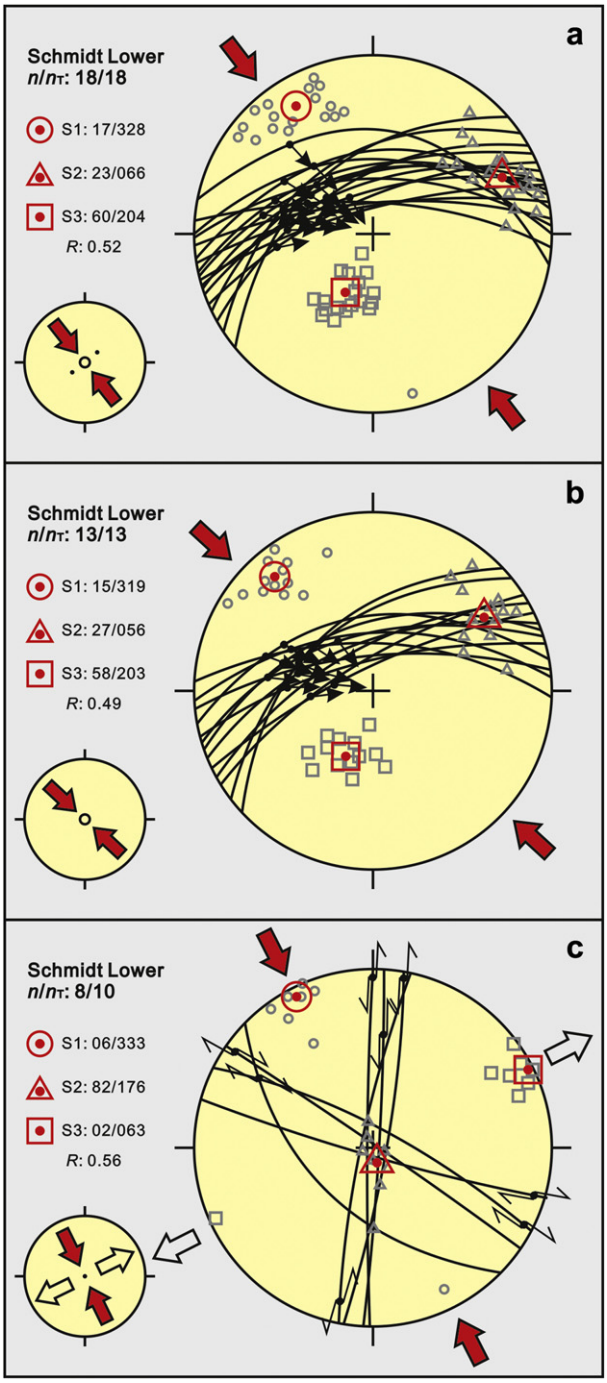

Figure 5 Graphical solutions of palaeostress tensors in the Fukang–Tianchi route. Slip lines: black dot with outward arrow for normal faulting, inward arrow for reverse faulting and double arrows for strike-slip faulting. Stress inversion results are represented by the orientation of the three principal stress axes; a dot surrounded by a circle for σ_1, a triangle for σ_2, and a square for σ_3. The related S_{Hmax} and S_{hmin} are represented by large arrows outside the stereogram. White arrows when σ_3 is subhorizontal (always S_{hmin}), green arrows when σ_2 is subhorizontal (either S_{hmin} or S_{Hmax}), red arrows when σ_1 is subhorizontal (always S_{Hmax}). Outward arrow indicates extensional deviatoric stress and inward arrow indicates compressional deviatoric stress.

might record the Mesozoic tectonic stress field based on the maximum principal stress direction (Table 1 and Fig. 5).

According to the analysis above, the direction of maximum principal stress axes (σ_1) in the southern edge of Junggar Basin during the end Late Paleozoic period is estimated as NW–SE (Figs. 3, 5 and 6; Table 1).

4. Discussion

4.1. Stress regimes

The stress regimes can be used to define the tensor type (Delvaux et al., 1995, 1997). The stress regime is defined by the vertical stress axes; if σ_1 is vertical, it is extensional, and if σ_2 is, then it is strike-slip, and it is compressive if the vertical axes is σ_3. Furthermore, the stress regime has a relation with the ratio of principal stress differences R (Fig. 7).

The stress index R' is defined from a combination of the stress ratio R and the nature of the most vertical principal stress axes (Delvaux et al., 1997; Delvaux and Sperner, 2003), and it can define all types of stress regimes systematically. It is ranging from 0 to 3 as follows: $R' = R$ when σ_1 is vertical (extensional stress regime), $R' = 2 - R$ when σ_2 is vertical (strike-slip stress regime) and $R' = 2 + R$ when σ_3 is vertical (compressive stress regime) (Delvaux et al., 1997; Delvaux and Sperner, 2003; Zhang and Wang, 2004).

A continuous scale ranging from 0 to 1 is defined for normal faulting regimes, from 1 to 2 for strike-slip regimes and from 2 to 3 for thrust faulting regimes (Delvaux et al., 1995; Delvaux and Barth, 2010).

The stress index R' in the study is about 1.44 to 2.52 (Table 2), with an average of 2.09, suggesting variation from strike-slip to compressive stress regime in the southern edge of Junggar Basin during the end Late Paleozoic.

The angle of σ_3 calculated from the faults is inclined up to 31 degrees in average from the vertical (Figs. 5 and 6), which may indicate there is the action of shearing traction acting along the air-earth interface to some extent. Therefore, at shallow depths, the angle σ_3 need not to be perpendicular to the earth's surface. The angle of axial plane of folds also shows the existence of little shearing traction (Fig. 5).

4.2. Driving force

During the Late Carboniferous to Early Permian, only a remnant part of the Junggar Ocean was still in the subduction in the inner part of the orocline (Xiao et al., 2010). The closure of the basin was accommodated by the development of strike-slip faults and dextral kinematics in Tianshan (Laurent-Charvet et al., 2003; Wang et al., 2007) and sinistral kinematics in Altai (Charvet et al., 2007).

The end of Paleozoic is characterized by transcurrent tectonics. Since the Permian, sinistral strike-slip along the Irtysh fault and dextral strike-slip along the Tianshan shear zones accommodated the counterclockwise rotation of south Junggar with respect to Siberia (Wang et al., 2007; Choulet et al., 2010; Fig. 8); and the accommodated motion was completed till Cretaceous and possibly Middle Triassic time (Lyons et al., 2002). Therefore, the accommodated rotation among these plates might cause this stress field in the study area and even in the whole Junggar terrain during the end Late Paleozoic.

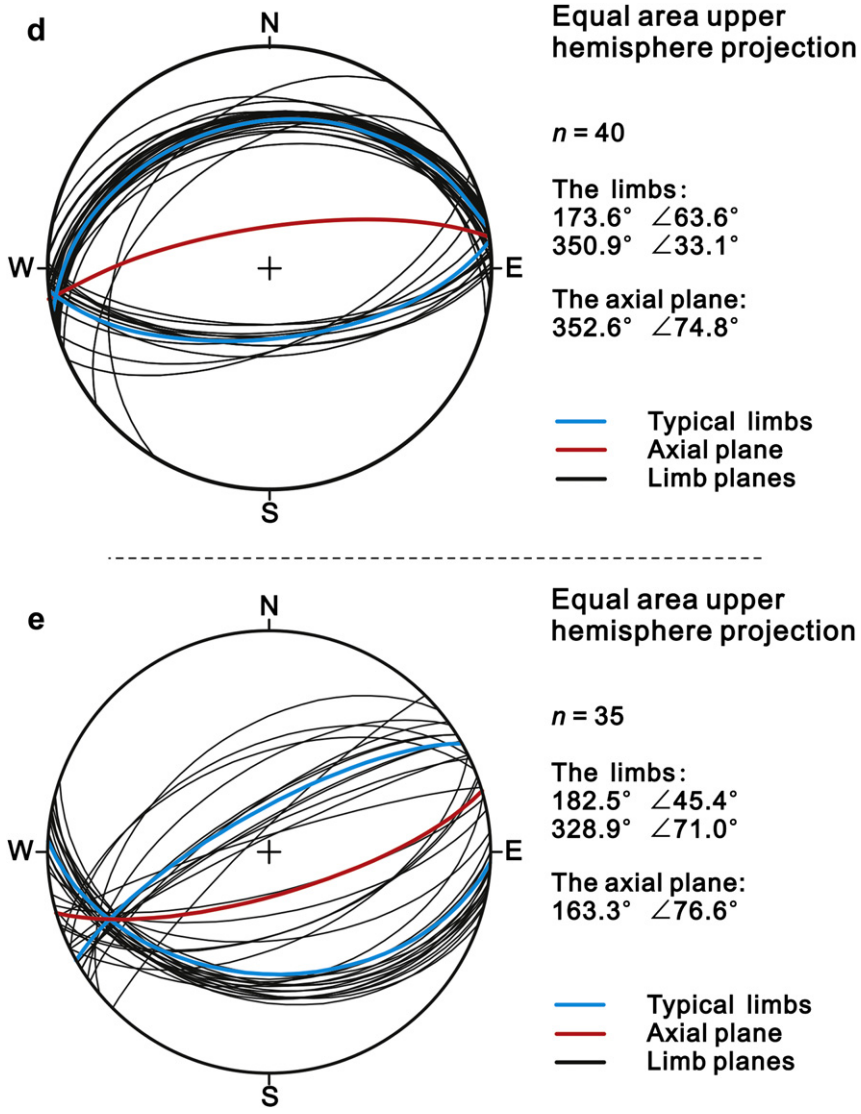

Figure 5 (*continued*).

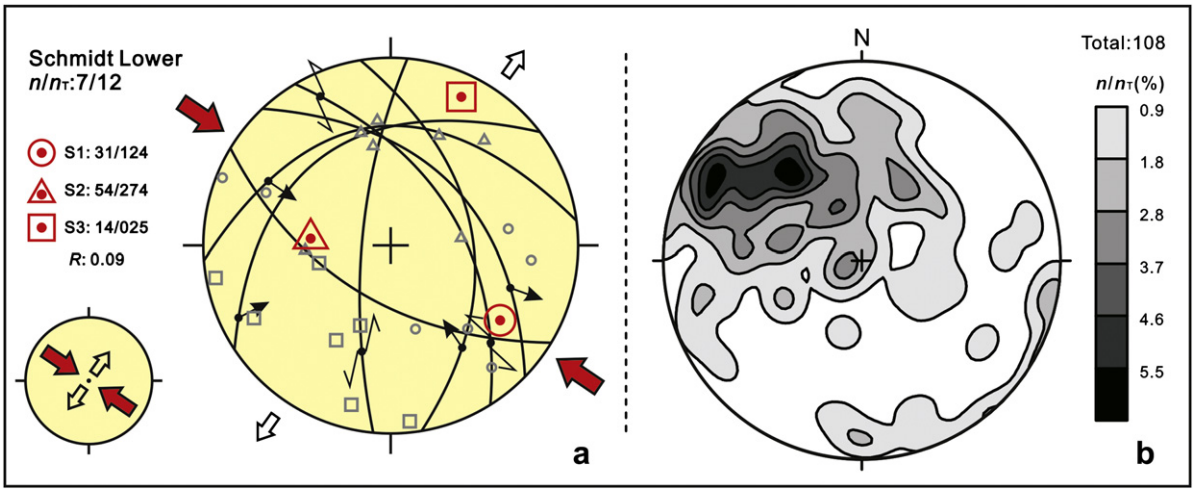

Figure 6 Graphical solutions of palaeostress tensors in the Urumqi–Tuoli route. a: faults with slickensides in the Carboniferous strata of the Urumqi–Tuoli route; b: isodensity map of the maximum principal stress derived from conjugate joints, south of Tuoli County (Xiao et al., 2009).

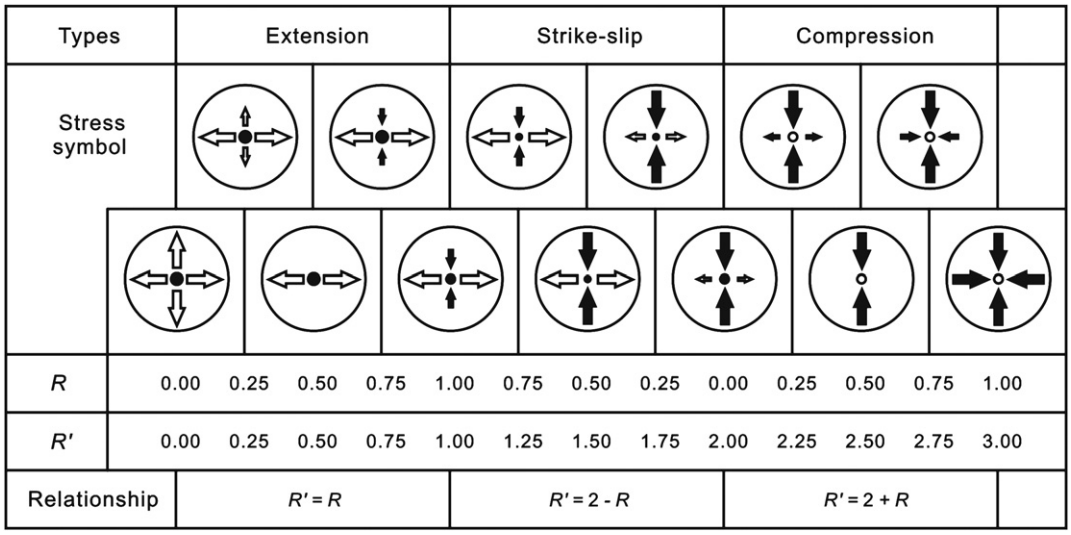

Figure 7 Types of stress regimes and their representation in map view (after Delvaux et al., 1995). Arrows indicate the azimuth of horizontal stress axes, with their length according to the relative stress magnitude. While outward arrows indicate extensive deviatoric stress axes and black inwards arrows indicate compressive deviatoric stress axes. Vertical stress axes are symbolized by a solid circle for extensive regimes (σ_1 vertical), a dot for strike-slip regimes (σ_2 vertical) and an empty circle for compressive regimes (σ_3 vertical).

Table 2 Stress inversion results of fault plane with slickensides and conjugate joints.

Box definition			Tectonic stress regime			Horizontal stress axes SH	
Site	Types	Number	Regime	R	R'	S_{Hmax}	S_{hmin}
FT01	1	18	TF	0.52	2.52	131	041
FT02	1	13	TF	0.49	2.49	132	042
FT03	2	10	SS	0.56	1.44	163	073
UT	1	12	SS	0.09	1.91	128	038

The stress regime: NF, normal faulting; SS, strike-slip faulting; TF, thrust faulting; NS, intermediate between NF and SS; TS, intermediate between SS and TF. Date type: 1 — fault plane with slickensides; 2 — conjugate joints.

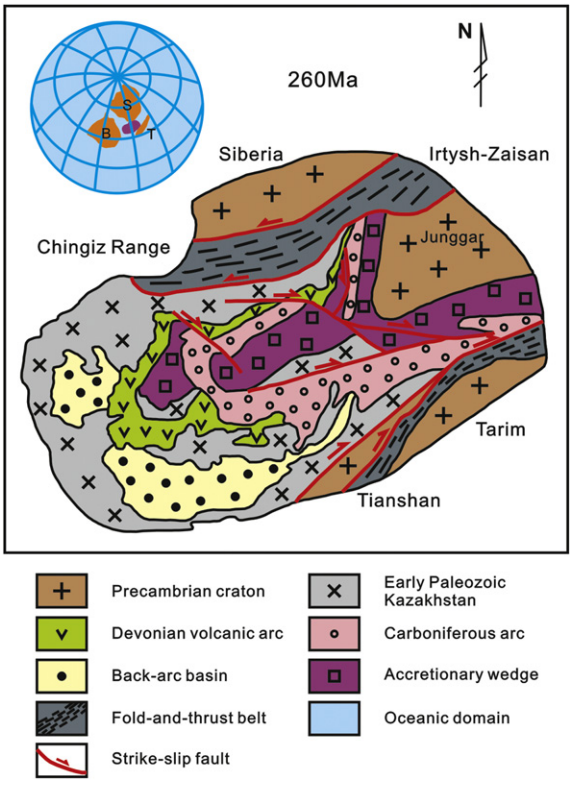

Figure 8 Tectonic map of Eastern Central Asia during the end Late Paleozoic period (after Van der Voo et al., 2008).

5. Conclusions

The tectonic stress field in southern edge of Junggar Basin is reconstructed with stress-response structures (dykes, conjugate joints, faults with slickenside and folds), the average occurrence of maximum (σ_1) principal compressive stress is 16/324 (dip angle/strike), the average intermediate (σ_2) principal compressive stress is 25/62 (dip angle/strike), and the average minimum (σ_3) principal compressive stress is 59/203 (dip angle/strike). The accommodated motion among plates is inferred to be the cause of this stress field in the southern edge of Junggar Basin during the end Late Paleozoic.

The stress index R' in the study area is about 1.44 to 2.52, with an average of 2.09, thus the stress regime of the southern edge of Junggar Basin is a variation from strike-slip to compressive.

The reconstruction of the tectonic stress field in the southern edge of Junggar Basin at the end Late Paleozoic provides insights into the tectonic deformation processes around the southern Junggar Basin and sheds light on a further understanding of the basin evolution and tectonic settings during that period.

Acknowledgements

This study was supported by the National Natural Science Foundation of China Grant (Nos. 40772121, 40314141 and 40172066) and China National Project 973 (No. 2009CB219302). Many thanks to Prof. M. Santosh, as well as Prof. Jinjiang Zhang, Prof.

Shuguang Song and Prof. Bei Xu of Peking University, China, for constructive suggestions, and we also would like to express our gratitude to two reviewers Prof. Wenjiao Xiao and Prof. Dilip Saha who considerably improve this article.

References

Angelier, J., 1979. Determination of the mean principal directions of stresses for a given fault population. Tectonophysics 56, T17–T26.

Angelier, J., 1989. From orientation to magnitudes in palaeostress determinations using fault slip data. Journal of Structural Geology 11, 37–50.

Arlegui, L., Simon, J.L., 2001. Geometry and distribution of regional joint sets in a non-homogeneous stress filed: case study in the Ebro basin (Spain). Journal of Structural Geology 23, 297–313.

Bott, M.H.P., 1959. The mechanisms of oblique slip faulting. Geological Magazine 96, 109–117.

Cao, C.J., 2005. Tectonic stress field analysis and application in the northwest Sichuan basin. Ph.D thesis, Chinese Academy of Geological Sciences, Beijing, 116 pp (in Chinese with English abstract).

Charvet, J., Shu, L.S., Laurent-Charvet, S., 2007. Paleozoic structural and geodynamic evolution of eastern Tianshan (NW China): welding of the Tarim and Junggar plates. Episodes 30, 162–186.

Chen, F.J., Wang, X.W., Wang, X.W., 2005. Prototype and tectonic evolution of the Junggar basin, northwestern China. Earth Science Frontiers 12 (3), 77–89 (in Chinese with English abstract).

Chen, X., Lu, H.F., Shu, L.S., Wang, H.M., Zhang, G.Q., 2002. Study on tectonic evolution of Junggar basin. Geological Journal of China Universities 8 (3), 257–267 (in Chinese with English abstract).

Chen, Y.Q., Wang, W.F., 2004. Geodynamics process in the Junggar basin. Journal of Geomechanics 10 (2), 155–164 (in Chinese with English abstract).

Choulet, F., Chen, Y., Wang, B., Faure, M., Cluzel, D., Charvet, J., Lin, W., Xu, B., 2010. Late Paleozoic paleogeographic reconstruction of Western Central Asia based upon paleomagnetic data and its geodynamic implications. Journal of Asian Earth Sciences 42 (5), 867–884.

Choulet, F., Faure, M., Cluzel, D., Chen, Y., Lin, W., Wang, B. From oblique accretion to transpression in the evolution of the Altaid collage: new insights from West Junggar, northwestern China. Gondwana Research, in press. doi:10.1016/j.gr.2011.07.015.

Delvaux, D., 1993. Quaternary stress evolution in East Africa from data of the western branch of the East African rift. In: Thorweihe, Schandelmeier (Ed.), Geoscientific Research in Northern Africa. Balkema, Rotterdam, pp. 315–318.

Delvaux, D., Barth, A., 2010. African stress pattern from formal inversion of focal mechanism data. Tectonophysics 482, 105–128.

Delvaux, D., Moeys, R., Stapel, G., Melnikov, A., Ermikov, V., 1995. Palaeostress reconstruction and geodynamics of the Baikal region, Central Asia, Part 1. Palaeozoic and Mesozoic pre-rift evolution. Tectonophysics 252, 61–101.

Delvaux, D., Moeys, R., Stapel, G., Petit, C., Levi, K., Miroshnichenko, A., Ruzhich, V., Sankov, V., 1997. Palaeostress reconstruction and geodynamics of the Baikal region, Central Asia, Part 2. Cenozoic rifting. Tectonophysics 282, 1–38.

Delvaux, D., Sperner, B., 2003. Stress tensor inversion from fault kinematic indicators and focal mechanism data: the TENSOR program. In: Nieuwland, D. (Ed.), New Insights into Structural Interpretation and Modeling. Geological Society, London Special Publications, pp. 75–100.

Doblas, M., 1998. Slickenside Kinematic Indicators. In: Rock Deformation: The Logan Volume. Elsevier, Amsterdam, Netherlands, pp. 187–197.

Ernst, R.E., Grosfils, E., Mege, D., 2001. Gaint dyke swarms on Earth, Venus, and Mars. Annual Review of Earth and Planetary Sciences 29, 489–534.

Ernst, R.E., Head, J.W., Parfitt, E., Grosfils, E., Wilson, L., 1995. Giant radiating dyke swarms on Earth and Venus. Earth Science Review 39, 1–58.

Etchecopar, A., Vasseur, G., Daigniers, M., 1981. An inverse problem in microtectonics for the determination of stress tensors from fault striation analysis. Journal of Structural Geology 3, 51–65.

Eyal, Y., Gross, M.R., Engelder, T., Becker, A., 2001. Joint development during fluctuation of the regional stress field in southern Israel. Journal of Structural Geology 23, 279–296.

Ferroni, A.C., Levi, N., Ottria, G., 2008. Duplex architecture and late-orogenic back thrusting in Foredeep Units of the Northern Apennines (Italy). Geological Journal 43, 447–462.

Foeken, J.P.T., Bertotti, G., Dunai, T.J., 2006. The morphology of a Messinian valley and its hinterland (Ventimiglia, NW Italy): a Miocene to Pliocene reconstruction. Geological Journal 41 (5), 465–480.

Geng, H.Y., Sun, M., Yuan, C., Xiao, W.J., Xian, W.S., Zhao, G.C., Zhang, L.F., Wong, K., Wu, F.Y., 2009. Geochemical, Sr–Nd and zircon U–Pb–Hf isotopic studies of Late Carboniferous magmatism in the West Junggar, Xinjiang: implications for ridge subduction? Chemical Geology 266, 364–389.

Gudmundsson, A., 1995. The geometry and growth of dykes. In: Baer, G., Heimann, A. (Eds.), Physics and Chemistry of Dykes. Balkema, Rotterdam, Netherlands, pp. 23–34.

Han, B.F., He, G.Q., Wang, S.G., 1999. Post-collision mantle-derived magmatism, underplating and the nature of Junggar basin basement. Science in China (Series D) 29 (1), 16–21 (in Chinese with English abstract).

Hoek, J.D., Seitz, H.M., 1995. Continental mafic dyke swarms as tectonic indicator: an example from the Vestfold Hills, East Antarctica. Precambrian Research 75, 121–139.

Hou, G.T. Mechanism for three types of mafic dyke swarms. Geoscience Frontiers, in press. doi:10.1016/j.gsf.2011.10.003.

Hou, G.T., Kusky, T.M., Wang, C.C., Wang, Y.X., 2010a. Mechanics of the giant radiating Mackenzie dyke swarm: a palaeostress field modeling. Journal of Geophysical Research 115 B02402.

Hou, G.T., Li, J.H., Jin, A.W., Qian, X.L., 2005. The Precambrian basic dyke swarms in the western Shandong Province. Acta Geologica Sinica 79 (2), 190–200 (in Chinese with English abstract).

Hou, G.T., Wang, C.C., Li, J.H., Qian, X.L., 2006. Late paleoproterozoic extension and a palaeostress field reconstruction of the North China Craton. Tectonophysics 422, 89–98.

Hou, G.T., Wang, Y.X., Hari, K.R., 2010b. The late Triassic and late Jurassic stress fields and tectonic transmission of North China Craton. Journal of Geodynamics 50, 318–324.

Laurent-Charvet, S., Charvet, J., Monie, P., Shu, L.S., 2003. Late Paleozoic strike-slip shear zones in eastern Central Asia (NW China): new structural and geochronological data. Tectonics 22, 1009.

Lyons, J.J., Coe, R.S., Zhao, X.X., Renne, P.R., Kazansky, A.Y., Izokh, A.E., Kungurtsev, L.V., Mitrokhin, D.V., 2002. Paleomagnetism of the early Triassic Semeitau igneous series, eastern Kazakstan. Journal of Geophysical Research-Solid Earth 107 (B7) EPM4-1–EPM4-15.

Manby, G.M., Lyberis, N., 1996. State of stress and tectonic evolution of the West Spitsbergen Fold Belt. Tectonophysics 267, 1–29.

Pirajno, F., Seltman, R., Yang, Y., 2011. A review of mineral systems and associated tectonic settings of northern Xinjiang, NW China. Geoscience Frontiers 2, 157–185.

Ramsay, J.G., Huber, M.I., 1987. The Techniques of Modern Structural Geology. In: Folds and Fractures, vol. 2. Academics Press, London, 700 pp.

Rawnsley, K.D., Peacock, D.C.P., Rives, T., Petit, J.P., 1998. Joints in the Mesozoic sediments around the Bristol Channel basin. Journal of Structural Geology 20 (12), 1641–1661.

Ray, R., Sheth, H.C., Mallik, J., 2007. Structure and emplacement of the Nandurbar-Dhule mafic dyke swarm, Deccan Traps, and the tectono-magmatic evolution of flood basalts. Bulletin of Volcanology 69, 537–551.

Tao, M.X., 1992. Characteristics of the Mesozoic and Cenozoic tectonic stress fields of the Urumqi-Usu region, Xinjiang. Acta Geologica Sinica 66 (3), 206–218 (in Chinese with English abstract).

Van der Voo, R., Abrajevitch, A., Bazhenov, M.L., Levashova, N.M., 2008. A Late Paleozoic Orocline that Developed in the Central Asian Triangle between the Converging Baltica, Siberia and Tarim Cratons. 33rd International Geological Congress, Oslo.

Wan, T.F., 1988. Palaeotectonic Stress Field. Geological Publishing House, Beijing, 152 pp (in Chinese).

Wang, B., Chen, Y., Zhan, S., Shu, L.S., Faure, M., Cluzel, D., Charvet, J., Laurent-Charvet, S., 2007. Primary Carboniferous and Permian paleomagnetic results from the Yili Block (NW China) and their implications on the geodynamic evolution of Chinese Tianshan Belt. Earth and Planetary Science Letters 263, 288−308.

Wang, W.F., Chen, Y.Q., 2004. Tectonic evolution and petroleum systems in the Junggar basin. Acta Geologica Sinica 78 (3), 667−675.

Wu, K.Y., Cha, M., Wang, X.L., Qu, J.X., Chen, X., 2005. Further researches on the tectonic evolution and dynamic setting of Junggar basin. Acta Geoscientica Sinica 26 (3), 217−222 (in Chinese with English abstract).

Wu, X.Z., Wang, L.H., Song, Z.L., 2000. The relations between the structural stress field and hydrocarbon migration and accumulation in southern margin of Junggar basin. Xinjiang Petroleum Geology 21 (2), 97−100 (in Chinese with English abstract).

Xiao, F.F., Hou, G.T., Wang, Y.X., Li, L., 2009. Study on structural stress field since Permian, Junggar basin and adjacent areas. Acta Scientiarum Naturalium Universititatis Pekinensis 3, 37−43 (in Chinese with English abstract).

Xiao, W.J., Han, C.M., Yuan, C., Sun, M., Lin, S.F., Chen, H.L., Li, Z.L., Li, J.L., Sun, S., 2008. Middle Cambrian to Permian subduction-related accretionary orogenesis of Northern Xinjiang, NW China: implications for the tectonic evolution of Central Asia. Journal of Asian Earth Sciences 32, 102−117.

Xiao, W.J., Huang, B.C., Han, C.M., Sun, S., Li, J.L., 2010. A review of the western part of the Altaids: a key to understanding the architecture of accretionary orogens. Gondwana Research 18, 253−273.

Xiao, Y., Zhang, H., Shi, J., Su, B., Sakyi, P.A., Lu, X., Hu, Y., Zhang, Z., 2011. Late Paleozoic magmatic record in East Junggar, NW China and its significance: implication from zircon U−Pb dating and Hf isotope. Gondwana Research 20, 532−542.

Xiao, X.C., 1992. The Tectonics of North Xinjiang and Adjacent Areas. Geological Publishing House, Beijing, 169 pp (in Chinese).

Yang, X.F., He, D.F., Wang, Q.C., Tang, Y., Tao, H.F., Li. D. Provenance and tectonic setting of the Carboniferous sedimentary rocks of the East Junggar Basin, China: evidence from geochemistry and U−Pb zircon geochronology. Gondwana Research, in press. doi:10.1016/j.gr.2011.11.001.

Zaineldeen, U., Delvaux, D., Jacobs, P., 2002. Tectonic evolution in the Wadi Araba segment of the Dead Sea Rift, South-West Jordan. European Geophysical Society (Special Publication Series) 2, 63−81.

Zhang, G.J., 1995. Review and outlook on petroleum exploration in Junggar basin. Journal of Xinjiang Petroleum Geology 16 (3), 196−199 (in Chinese with English abstract).

Zhang, J.E., Xiao, W.J., Han, C.M., Ao, S.J., Yuan, C., Sun, M., Geng, H.Y., Zhao, G.C., Guo, Q.Q., Ma, C., 2011. Kinematics and age constraints of deformation in a late Carboniferous accretionary complex in Western Junggar, NW China. Gondwana Research 19, 958−974.

Zhang, L., Jiang, Z.X., Guo, Z.T., 2007. Relationship between structural stress and hydrocarbon bearing pool formation. Natural Gas Geoscience 18 (1), 32−36 (in Chinese with English abstract).

Zhang, Z.P., Wang, Q.C., 2004. The summary and comment on fault-slip analysis and palaeostress reconstruction. Advances in Earth Science 19 (4), 605−613 (in Chinese with English abstract).